# Long term process-based morphological model of the Western Scheldt Estuary

G. Dam & A.J. Bliek
*Svašek Hydraulics, Rotterdam, The Netherlands*

R.J. Labeur
*Delft University of Technology, Delft, The Netherlands*

S. Ides & Y. Plancke
*Flanders Hydraulic Research, Antwerp, Belgium*

ABSTRACT: A process-based morphological model of the Western Scheldt Estuary based on the finite elements method is presented in this paper. This model is able to successfully hindcast the morphological developments of the Western Scheldt over several decades. The measured sedimentation/erosion pattern versus the pattern calculated by FINEL2d over the period 1965 – 2002 was compared. Good agreement was found in overall patterns, although many differences were still to be seen in detail. It was concluded that the model can be used to evaluate different scenarios, making it a useful tool for decision making processes e.g. future deepenings of the fairway.

## 1 INTRODUCTION

The Western Scheldt estuary lies in the south-western part of the Netherlands and is the gateway to the port of Antwerp. A large amount of dredging is necessary to maintain the required depth of the navigation channel to the port of Antwerp.

The morphological developments of this estuary are complex and are governed by natural processes and by human interventions. Since a lot of functions in the Western Scheldt are related to morphology the need for predicting future developments is high. Until now long term morphological predictions were carried out by using (semi)-empirical models, like ESTMORF (Wang et al., 1999). Process-based morphological models were not yet able to reproduce the morphological development very well over decades, partly because of the large amount of computational time involved. Hibma et al., (2003) uses a process-based morphological model with a conceptual model of an estuary like the Western Scheldt.

In this paper a process-based morphological model FINEL2d is presented which is used to reproduce the morphological developments of this estuary during the last decades. A previous successful study prepared with FINEL2d is carried out in the Haringvliet estuary (Dam, et al., 2005).

The calibration of the model was carried out in consecutive parts. A first stage consisted of a calibration of the water motion, next the morphological module was calibrated over the period 1995 until 2002. The calibrated model was then validated from 1965 until 2002.

The content of this paper is as follows: In section 2 the Western Scheldt estuary is introduced. Section 3 describes the FINEL2d model. The model set-up of the Western Scheldt model is discussed in section 4. Section 5 presents the morphological results. Finally in section 6 some conclusions are given.

## 2 THE WESTERN SCHELDT ESTUARY

The Western Scheldt estuary is a dynamic system that has gone through may changes due to human impacts and natural developments. The morphology of the Western Scheldt is very important for all functions related to this area, e.g. navigation, ecology and sand mining.

The vertical tide in the Western Scheldt ranges from an average 3.9 m in the mouth to 5.0 m near Antwerp. Fresh water discharge from the River Scheldt is limited compared to the tidal volumes.

The Western Scheldt estuary is a multiple channel system. The tidal flats and surrounding ebb and flood channels form morphological macro cells. The entire Western Scheldt consists of such morphological cells, see Figure 1. At the locations where the cells coincide, sills develop, which block the fairway to the port of Antwerp and therefore require regular dredging (Winterwerp et al., 2001).

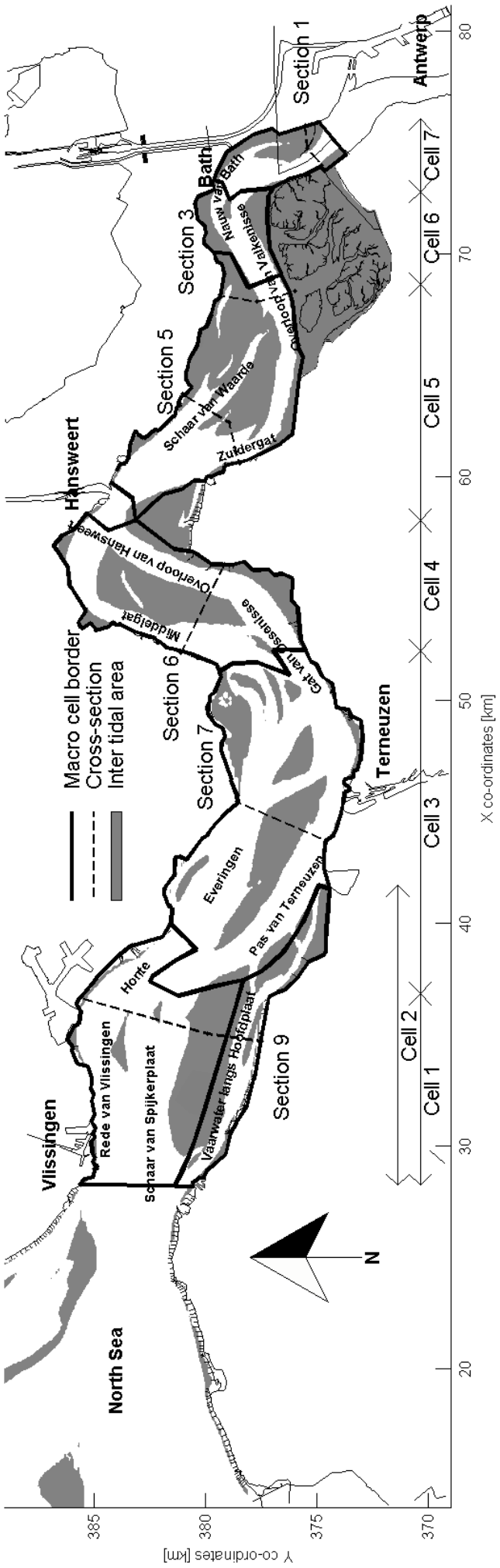

Figure 1: Layout of the Western Scheldt Estuary

In the 1970's and 1990's a deepening of the navigational channel has been carried out to allow vessels with greater draught to enter the port of Antwerp. Most of the dredging had to be done at these sills. The dredging volumes (maintenance plus deepening) range from 5 $Mm^3$ in 1968 to 14 $Mm^3$ during the second deepening. After the second deepening the volumes seem to establish around 7 to 8 $Mm^3$ per year. The dredged material is deposited into the estuary in especially designated areas, usually in the secondary branches.

Sand mining also plays a role in the Western Scheldt. Yearly approximately 2.0 to 2.5 $Mm^3$ sand is mined. In contradiction to channel dredging this sand is really extracted from the estuary.

The Western Scheldt consists mainly of fine non-cohesive sediments; only at inter tidal areas silt can be found. In the model only non-cohesive sediment is taken into account.

Since the Western Scheldt is fairly sheltered from the waves of the North Sea the morphological development is mainly tidal driven and waves are neglected in this study.

## 3 THE MORPHODYNAMIC MODEL FINEL2D

### 3.1 *General*

FINEL2d is a 2DH numerical model based on the finite elements method and is developed by Svašek Hydraulics. The following sections describe the governing equations of the FINEL2d model.

### 3.2 *Hydrodynamic module*

The depth-integrated shallow water equations are the basis of the flow module. For an overview on shallow water equations see Vreugdenhil (1994).

The model equations are the continuity equation:

$$\frac{\partial h}{\partial t} + \frac{\partial uD}{\partial x} + \frac{\partial vD}{\partial y} = 0, \tag{1}$$

the x-momentum balance:

$$\frac{\partial Du}{\partial t} + \frac{\partial Du^2}{\partial x} + \frac{\partial Duv}{\partial y} + f_c Dv + gD\frac{\partial h}{\partial x} - \frac{1}{\rho}\tau_{x,b} + \frac{1}{\rho}\tau_{x,w} + \frac{1}{\rho}\tau_{x,r} = 0, \tag{2}$$

and the y-momentum balance:

$$\frac{\partial Dv}{\partial t} + \frac{\partial Duv}{\partial x} + \frac{\partial Dv^2}{\partial y} - f_c Du + gD\frac{\partial h}{\partial y} - \frac{1}{\rho}\tau_{y,b} + \frac{1}{\rho}\tau_{y,w} + \frac{1}{\rho}\tau_{y,r} = 0. \tag{3}$$

where $u$=depth averaged velocity in x-direction [m/s]; $v$=depth averaged velocity in y-direction [m/s]; $h$=water level [m]; $z_b$=bottom level [m]; $D$=water depth [m]; $f_c$=Coriolis coefficient [1/s]; $g$=gravitational acceleration [m/s$^2$]; $\rho$=density of water [kg/m$^3$]; $\tau_b$=bottom shear stress [N/m$^2$]; $\tau_w$=wind shear stress [N/m$^2$]; and $\tau_r$=radiation stress [N/m$^2$];

In addition to the effect of advection and pressure gradients, external forces like the Coriolis force, bottom shear stress, wind shear stress and radiation stress due to surface waves can be taken into account. It is noted that turbulent shear stresses are not taken into account: the application is therefore restricted to advection dominated flows only.

As a solution method, the discontinuous Galerkin method is adopted (Hughes, 1987) in which the flow variables are taken constant in each moment. This method has advantages in dealing with drying elements.

As the momentum equations contain first order derivatives in space, they can be written as:

$$\frac{\partial \boldsymbol{U}}{\partial t} + \nabla \cdot \boldsymbol{F} = \boldsymbol{H} \tag{4}$$

where:

$$\boldsymbol{U} = \begin{pmatrix} h \\ uD \\ vD \end{pmatrix}, \quad \boldsymbol{F} = \begin{pmatrix} uD & vD \\ u^2D + \frac{1}{2}gh^2 & uvD \\ uvD & v^2D + \frac{1}{2}gh^2 \end{pmatrix}, \quad \boldsymbol{H} = \begin{pmatrix} 0 \\ \frac{1}{\rho}\tau_{x,tot} - f_c vD - gDi_{b,x} \\ \frac{1}{\rho}\tau_{y,tot} + f_c uD - gDi_{b,y} \end{pmatrix} \tag{5}$$

in which $\tau_{tot,x}$ and $\tau_{tot,y}$ are summations of the external stresses in x- and y-direction respectively, while $\imath_{b,x}$ and $\imath_{b,y}$ are the bed level gradients in x- and y-direction respectively. The equation can be integrated over an element resulting in:

$$\int_{\Omega_e} \frac{\partial \boldsymbol{U}}{\partial t} \mathrm{d}\Omega + \int_{\Gamma_e} \boldsymbol{F}\,\boldsymbol{n}\,\mathrm{d}\Gamma = \int_{\Omega_e} \boldsymbol{H}\,\mathrm{d}\Omega, \tag{6}$$

where $\Omega_e$ denotes an element, $\Gamma_e$ the associated element boundary,while $\boldsymbol{n}$ is the outward pointing vector normal to $\Gamma_e$.

The problem is now reduced to the determination of the fluxes $\boldsymbol{F}$ along the boundaries. As the variables are determined at the elements and not at the sides, the flux F is not known beforehand, but involves the solution of a local Riemann problem. An approximate Riemann solver according to Roe (Glaister, 1993) is applied. This method guarantees strict mass and momentum conservation, but suffers from some numerical diffusion in stream-wise direction. An explicit time integration scheme is used. As this method restricts the time step, the time step is controlled automatically for optimum performance.

A special problem in shallow waters like for example estuaries is the drying and flooding of large areas during a tidal cycle. A discontinuous discretisation is used in combination with an explicit time-stepping. In this way this flooding and drying of the elements can be treated relatively easily. If an element tends to dry, the corresponding characteristic wave is partially reflected from this element which guarantees mass conservation.

### 3.3 *Sediment transport module*

FINEL2d uses the following sediment balance equation for the evolution of the bed level:

$$\frac{\partial z_b}{\partial t} + \frac{\partial q_x}{\partial x} + \frac{\partial q_y}{\partial y} = 0 \tag{7}$$

In which $z_b$ [m] is the bed level and $(q_x,q_y)$ [m$^2$/s] are the components of the sediment flux in x- and y-direction respectively.

In order to determine the non-cohesive part of the sediment fluxes, the transport formula of Engelund and Hansen formula is used (Engelund & Hansen, 1967). Since most of the sand transport in the Western Scheldt is suspended transport, a time lag effect is introduced in the model according to Gallapatti & Vreugdenhil (1985). First a dimensionless equilibrium concentration is calculated:

$$c_e = \frac{S}{D\sqrt{u^2 + v^2}} \tag{8}$$

where $c_e$ is equilibrium concentration [-] and $S$ the magnitude of the equilibrium sand transport [m$^2$/s] according to Engelund and Hansen.

The concentration $c$ [-] is then calculated according from:

$$\frac{dc}{dt} = \frac{1}{T_A}\left[c_e(t) - c(t)\right] \tag{9}$$

In which $T_A$ is a characteristic timescale [s].

Equation 9 shows that if the concentration is lower than the equilibrium concentration erosion will occur ($dc/dt > 0$). If the concentration is higher than the equilibrium concentration sedimentation will occur ($dc/dt < 0$). The coefficient $T_A$ characterises the time needed for the adjustment of the concentration and is

defined as $T_A = h/w_s$; where $w_s$ [m/s] is the settling velocity of the sand particles. In relative shallow areas the time scale is small and the concentration almost immediately adjusts to the equilibrium concentration.

## 4 MODEL SET UP

### 4.1 *Grid schematisation and boundary conditions*

FINEL2d uses unstructured triangular grids. The advantage of such meshes in comparison to for example finite difference grids, is the flexible mesh generation. In this way no nesting techniques are required in regions of specific interest, where a higher degree of resolution is needed, while arbitrary coastlines and complex geometries can be resolved very well.

The seaward boundaries of the computational mesh of the Western Scheldt are chosen approximately 40 km away from the coastline and coincide with the boundaries of existing models. The latter can be used to obtain the corresponding boundary conditions. A significant part of the river system in Belgium is also included in the schematisation. In Figure 2 the overall mesh is shown. In the area of interest, the Western Scheldt, the average grid size is approximately 1.1 ha. Near the seaward boundaries the grid size is approximately 2.5 km$^2$. The total number of elements (triangles) of the mesh is 44,111.

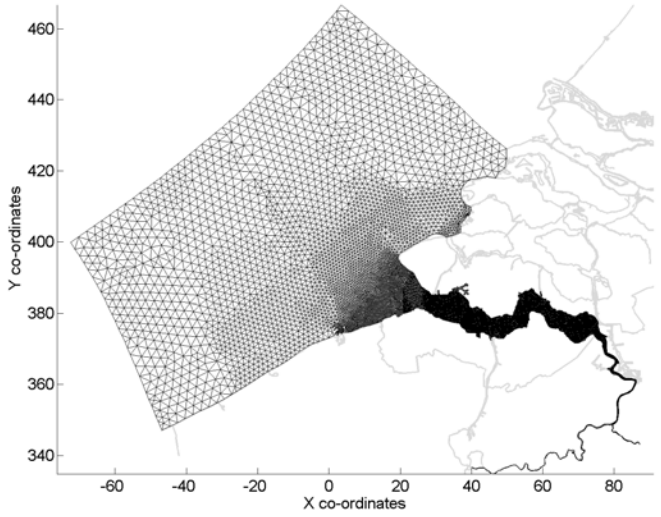


Figure 2: Computational mesh of the FINEL2d model

The river discharge at the river the Scheldt and the Rupel were taken constant at respectively 43 and 65 m$^3$/s.

### 4.2 *Calibration of the water motion*

The first step in the calibration of a morphodynamic model is to calibrate the water motion. In this model the water motion is mainly calibrated on measured water levels in the estuary. The calibration parameter is the bottom roughness. A trial and error method was used to find the optimal settings for the bottom roughness. An 8 day calibration period was chosen. In the mouth and the western part of the estuary a Nikuradse roughness height of 0.2 cm was found. The optimal roughness gradually increases from the west to the east of the estuary. In the east a Nikuradse roughness height of 10 cm was found. The difference between measured and computed high water, low water, tidal range and mid water level at the various water level stations are shown in Table 1. See Figure 1 for an overview of the water level stations.

Table 1. Water level deviations (cm)*

| Station | HW | LW | Tidal range | Mid |
|---|---|---|---|---|
| Vlissingen | -8 | -5 | -4 | -6 |
| Terneuzen | -7 | -9 | 2 | -8 |
| Hansweert | -3 | -12 | 9 | -7 |
| Bath | -6 | -10 | 3 | -8 |
| Antwerp | -2 | 4 | -6 | 1 |

* Averaged over a 8 day period;

The deviations are usually within a 10 cm accuracy range. With a tidal range of approximately 3 to 5 metres in the estuary this gives a deviation of only 3%.

The next step in the calibration of the water motion concerns the tidal volumes of various cross-sections in the estuary. The cross-sections have been surveyed from 2000 to 2002 using an acoustic current profiler during 13 hours. The same periods were simulated in the model. The results are summarised in Table 2 in which the flood and ebb tidal volume of both the measurement and the simulation are shown. See figure 1 for an overview of the cross-sections.

Table 2. Observed and simulated tidal volumes

| Cross-section Nr. | Name | Flood tidal volume O | M | M/O | Ebb tidal volume O | M | M/O* |
|---|---|---|---|---|---|---|---|
| 1b | Bath | 200 | 174 | 0.87 | 174 | 162 | 0.93 |
| 3b | Valkenisse | 288 | 270 | 0.94 | 275 | 264 | 0.96 |
| 5a | Waarde | 259 | 247 | 0.96 | 267 | 253 | 0.95 |
| 5b | Zuidergat | 160 | 159 | 1.00 | 151 | 147 | 0.97 |
| 6a | Ossenisse | 369 | 417 | 1.13 | 390 | 425 | 1.09 |
| 6b | Middelgat | 230 | 200 | 0.87 | 180 | 176 | 0.98 |
| 7a | Terneuzen | 344 | 347 | 1.01 | 417 | 383 | 0.92 |
| 7b | Everingen | 539 | 525 | 0.97 | 432 | 455 | 1.05 |
| 9a | Hoofdplaat | 112 | 112 | 1.00 | 113 | 105 | 0.93 |
| 9b | Spijkerplaat | 1051 | 1118 | 1.06 | 1063 | 1109 | 1.04 |

* O=observed volume [Mm$^3$]; M=model volume [Mm$^3$]; M/O is the model volume divided by the observed volume.

It is concluded that all observed discharges can be simulated with an accuracy of 15% and usually 10%. Finally, a comparison was made with current data at shallow banks and tidal flats. From the results of the of all calibration steps it can be concluded that the water motion is calibrated decisively.

### 4.3 *Morphological acceleration factor*

A morphological acceleration factor is used to multiply the calculated bottom changes to accelerate the computational time. A small morphological acceleration factor is preferred from a numerical point of view but is not practical because of the large computational time. In order to investigate the morphological acceleration factor several runs with different factors are carried out in the Western Scheldt model. The total amount of sedimentation and erosion volume after one year is calculated and compared to the calculation with a factor 1, since this is the run without any acceleration.

Table 3. Morphological acceleration factor.

| Factor | Sedimentation volume difference* | Erosion volume difference* |
|---|---|---|
| 1 | - | - |
| 5 | 7.6% | 8.4% |
| 24.75 | 10.3% | 14.6% |
| 49.5 | 48.1% | 43.2% |

* Difference is calculated relative to factor 1 and after 1 year.

From Table 3 it is concluded that if the acceleration factor is chosen higher the difference is increased as well. The acceleration factor used in this paper is 24.75. This factor shows a reasonable difference of less than 15% and gives reasonable computational times. This factor accelerates one neap spring tidal cycle to one year.

### 4.4 *Spiral flow*

In the 2DH flow model the effect of spiral flow in curved channels is neglected. In FINEL2d an option is present to include a parameterisation of the spiral flow. The formulation of Booij & Pennekamp (1983) has been used. The model calculates the curvature of the current. Based on this figure the direction of the sediment transport is adjusted.

In figure 3 the morphological effect of the spiral flow is shown for the Zuidergat area over the validation period from 1965 to 2002. As expected, the outer bend shows more erosion due to the spiral flow effect, while the inner bend shows sedimentation. The effect is approximately 5 metres in this channel. From Figure 3 it is concluded that spiral flow cannot be neglected in a morphological hindcast.

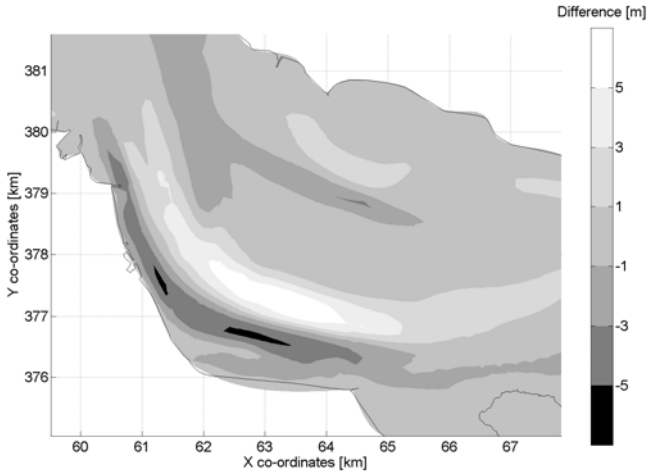


Figure 3: Morphological effect of spiral flow in Zuidergat area

### 4.5 *Dredging, depositing and sand mining module*

Dredging has a large impact on the morphodynamics in the Western Scheldt. Therefore this needs to be taken into account when performing a hindcast of the morphological developments of the last decades.

In reality a navigational depth is guaranteed between the navigational buoys of the fairway. If the depth becomes too shallow a dredger deepens the area to the required depth.

In FINEL2d a dredging module was developed based on the same principle. For each grid cell in the fairway a required depth is defined. If the depth in the grid cell is insufficient the sand is removed from the element and deposited according to a certain distribution key over depositing sites. The distribution key is established using historical data of the deposited material. For each historical year an input file is defined, since the buoys, the depositing areas and the maintained depth in the fairway may vary over the years.

Sand mining is simulated in the model by removing the mined volume equally spread over the specified sand mining area. Since sand mining quantities and locations differ per year an input file for each year is specified.

The morphodynamics of the estuary due to the combined effects of natural processes and dredge/depositing activities is continuously calculated, and the riverbed is accordingly updated.

### 4.6 *Calibration of the morphodynamics*

The next step in the set-up of the morphodynamic model is the calibration of the morphology itself. A calibration is carried out for a period of 7 years (1995-2002). Because the goal is to evaluate the

long term morphodynamics the calibration results will not be shown in this paper. See for details Dam et al., (2006). Only the optimal settings of the morphodynamic model found in the calibration are given in Table 4.

Table 4. Settings of the optimal calibration run.

| Factor | value | |
|---|---|---|
| Grain size | 150 | µm |
| Fall velocity of sand | 1.5 | cm/s |
| Morphological acceleration factor | 24.75 | [-] |
| Hydraulic roughness as described in section 4.2 | | |
| Spiral flow included as described in section 4.4 | | |
| Non erodable layers where relevant (situation of 2001) | | |
| Morphological start-up period | 1 | year |

## 5 MORPHODYNAMIC RESULTS

In the hindcast of the years 1965 to 2002 the settings found in the calibration period are used. Starting point is the bathymetry of 1964 and a start-up period of 1 year. This means that the model needs a start-up time to enable for the initialisation of the sand transport and the adaptation of the initial bottom, which was interpolated from GIS data. It was found that a start-up time of 1 year is sufficient to account for these factors.

The simulated erosion and sedimentation pattern of 1965 to 2002 is displayed in Figure 4 together with the observed pattern. At first sight a lot of similarities between the observed and simulated pattern occur. Macro cell 4 which is the Middelgat / Gat van Ossenisse system shows a good resemblance. The Middelgat is sedimentated, while the Gat van Ossenisse is eroded. Also the Zuidergat and the Overloop van Valkenisse shows good agreement.

Inter tidal areas are eroded too much in the model, maybe because in reality cohesive sediments can be found at these shoals, which can make it harder for these areas to erode.

At Cell 1 in the Schaar van Spijkerplaat a large sedimentation can be seen in the model, which in reality does not occur. A possible reason why the Schaar van Spijkerplaat is so heavily sedimentated is the neglecting of wave effects, which might still have a stirring effect in the mouth of the estuary. The waves also cause wave driven currents which might transport the sediment further eastwards with a dominant westward wave direction.

In Table 5 the sand volume changes in the macro cells of the hindcast period are shown. From Table 5 can be seen that the model calculates volume changes that are in order of magnitude of the observed volume changes. The Macro cells 3, 5, 6 and 7 are calculated quantitatively well by the model. In Cell 4 both channels show the right direction, but the sedimentation of the Middelgat channel is too less in the model. Cell 1 and 2 are not correctly calculated.

Table 5. Total sand volume changes 1965- 2002

| Cell Nr. | Flood channel | | Ebb channel | | Total | |
|---|---|---|---|---|---|---|
| | O | M | O | M | O | M * |
| 1 | -14 | 31 | 1 | 1 | -13 | 32 |
| 2 | | | | | 26 | 0 |
| 3 | -20 | -12 | -8 | -43 | -29 | -55 |
| 4 | -39 | -35 | 61 | 22 | 22 | -13 |
| 5 | 12 | 26 | -49 | -79 | -37 | -53 |
| 6 | -5 | -6 | -17 | -18 | -22 | -25 |
| 7 | -5 | -1 | -16 | -16 | -22 | -18 |
| 8 | | | | | 8 | -5 |
| 9 | | | | | -2 | 9 |
| Total | | | | | -68 | -127 |
| Sand mining | | | | | -100 | -100 |
| Nett | | | | | +32 | -27 |

* O =observed volume change [$Mm^3$]; M =modelled volume change [$Mm^3$]; negative =erosion, positive =sedimentation

The total sand volume change is calculated at –127 $Mm^3$ for the model while the measurements show a change of –68 $Mm^3$, see Table 5. Sand mining in this period extracted a total of 100 $Mm^3$ from the Western Scheldt estuary, which leads to a net export of sand of 27 $Mm^3$ in 37 years of the model. In reality there was an import of 32 $Mm^3$. This problem of import versus export needs to be solved in future research, because a lot of policy questions concerning the Western Scheldt are based on a possible change in export/import of sand. Note that the last years there seems to be an export of sand out of the Western Scheldt.

The effect of dredging and depositing is large in the Western Scheldt area. In Figure 5 the actual dredging volumes in the complete Western Scheldt are plotted along with the calculated dredging volumes of FINEL2d. As pointed out in section 2.6 the navigational depth of the shipping channel is guaranteed in the model. If the depth becomes too small the sand is removed and distributed over the depositing sites.

At first notice the model can reproduce the dredging volumes in an accurate way. Around 1974 a large peak in the dredging volumes occurs in the model. This is caused by the deepening of the fairway and the transfer of the fairway from the Middelgat to the Gat van Ossenisse channel.

Around 1996 a second deepening of the channel has taken place. This also causes an increase of the dredging volumes in both the model and in reality, but the model does not show dredging volumes as large as the 1970's deepening.

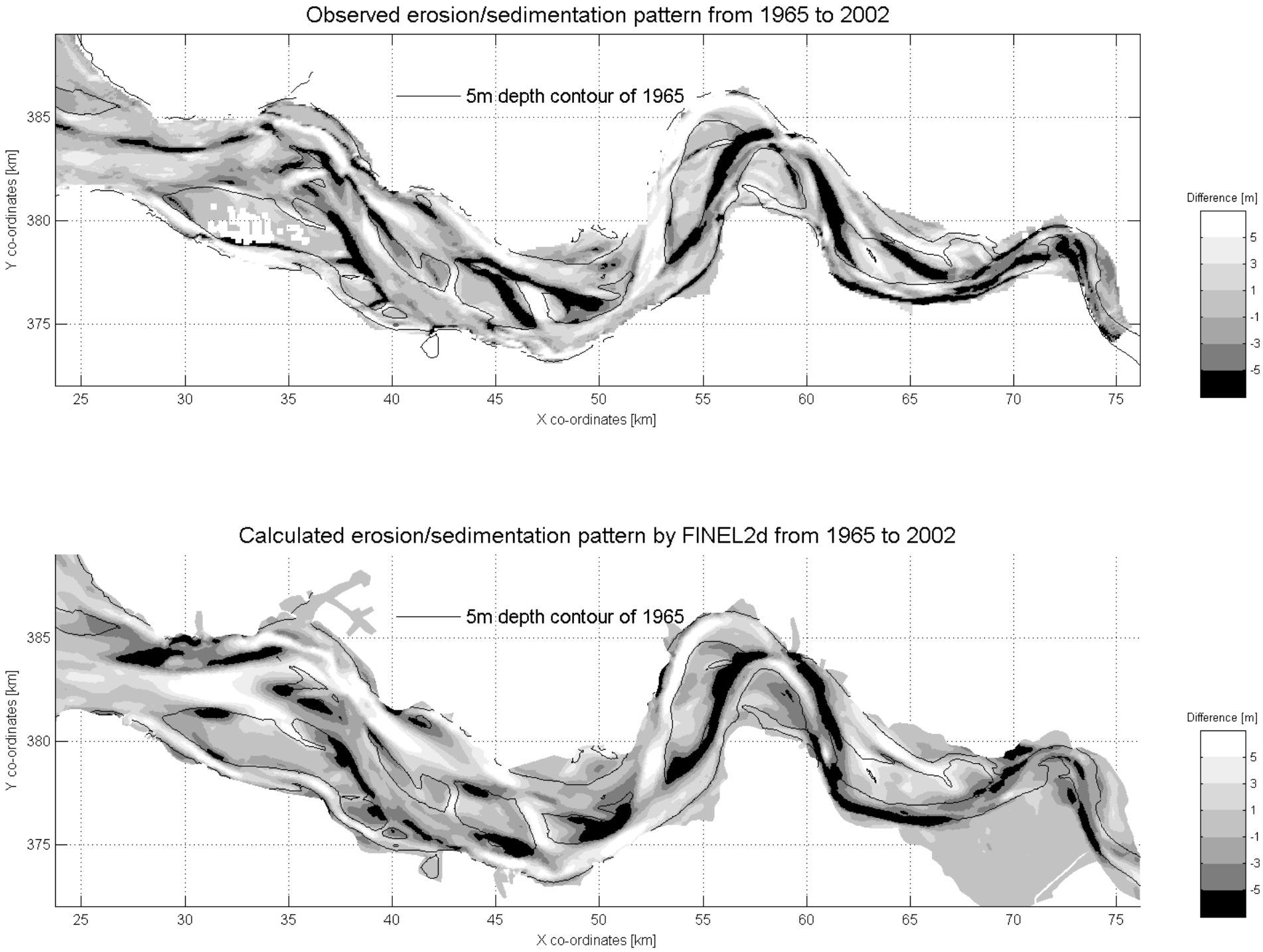


Figure 4: Observed versus calculated erosion/sedimentation pattern from 1965 to 2002

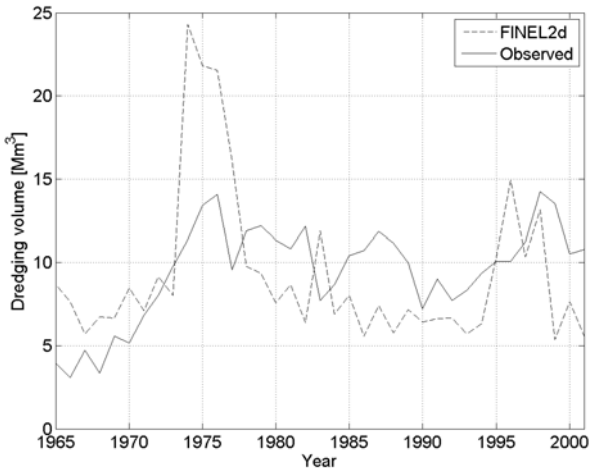


Figure 5: Observed and calculated total dredging volumes

In Figure 6 the simulated total dredging effort of the validation period is shown for the eastern part of the estuary, in which most of the dredging takes place. Also shown are the borders of the actual dredged areas. From Figure 6 it can be concluded that the location of the dredged material in the model gives a good agreement with reality.

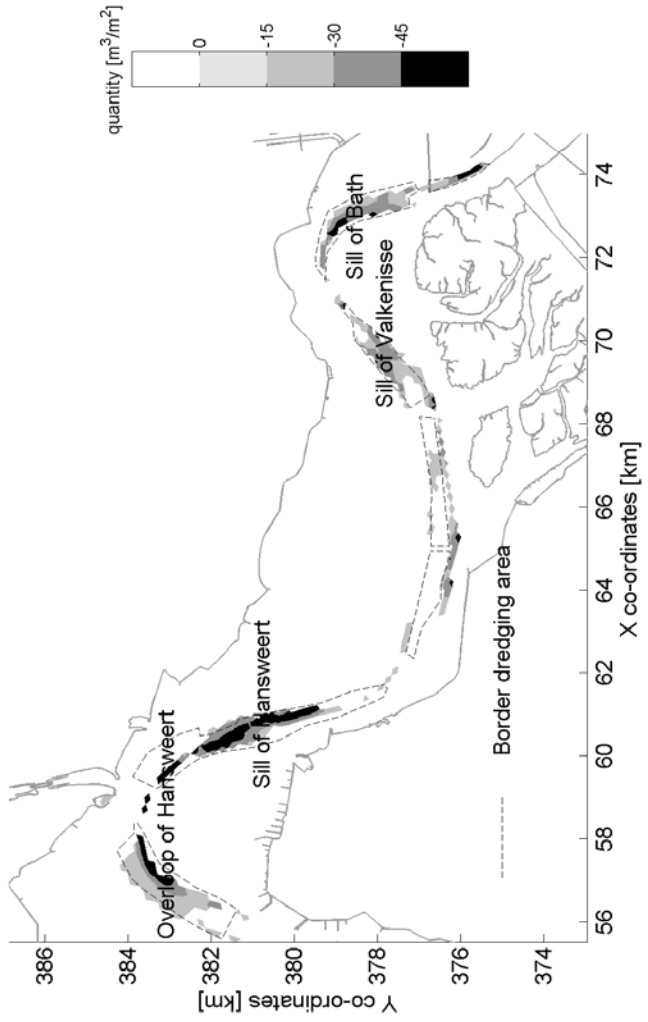


Figure 6: Calculated total dredging quantities [$m^3/m^2$]

## 6 CONCLUSION

The presented FINEL2d morphodynamic model of the Western Scheldt estuary is able to calculate the erosion/ sedimentation pattern fairly accurately over several decades. The results in the different macro cells still require optimisation, especially the import/ export of sand of the complete Western Scheldt. The dredging volumes can be reproduced in a fairly accurate way, although during the deepening of the fairway in the 1970's a further optimisation of this routine of the model is required.

It is concluded that the basis for a good long term process based morphological model is present. Further improvements of the model can be obtained by additional research. However in this state the model can already be used as a decision making tool for large scale human impacts in the Western Scheldt (e.g. further deepening of the fairway).

## REFERENCES

Booij, R., Pennekamp, Joh. G.S., 1983, Simulation of main flow and secondary flow in a curved open channel, Report No. 10-83, Department of Civil Engineering, Delft University of Technology.

Dam., G., Bliek, A.. J., Bruens, A. W., 2005, Band Width analysis morphological predictions Haringvliet Estuary, Proceedings of 4th IAHR symposium of the River, Coastal and Estuarine Morphodynamics Conference, Urbana, Illinois, USA, Volume 2, p. 171 –179.

Dam, G., Prooijen, B.C., van, Bliek. A.J., 2006, Morfodynamische berekeningen van de Westerschelde met behulp van FINEL2d (in Dutch), Svašek Hydraulics, ref. GD/06119/1339

Engelund, F., Hansen, E., 1967, A monograph on sediment transport in alluvial channels, Teknik Forlag, Copenhagen.

Gallappatti, R., Vreugdenhil, C. B., 1985, A depth-integrated model for suspended sediment transport. Journal of Hydraulic Research 23, p. 359-277.

Glaister, P. 1993. Flux difference splitting for open-channel flows, Int. J. Num. Meth. Fluids, 16, p. 629-654

Hibma, A., Vriend, H.J., de, Stive, M.J.F., 2003, Numerical modelling of shoal pattern formation in well-mixed elongated estuaries, Estuarine, Coastal and Shelf Science, Vol. 57, 5-6, p. 981-999

Hughes, T.J.R, 1987, The finite element method, Prentice-Hall, Englewood Cliffs, N.J.

Vreugdenhil, C.B., 1994, Numerical methods for shallow water flow, Institute for Marine and Atmospheric Research Utrecht (IMAU), Utrecht University, The Netherlands

Wang, Z.B., Langerak, A., Fokkink, R.J., 1999, Simulation of long-term morphological development in the Western Scheldt, Symposium of the International Association for Hydraulic Research, Genova, Italy.

Winterwerp, J. C., Wang, Z. B., Stive, M. J. F. Arends, A., Jeuken, C., Kuijper, C., Thoolen, P. M. C., 2001, A new morphological schematization of the Western Scheldt estuary, the Netherlands, Proceedings of the 2nd IAHR Symposium on River, Coastal and Estuarine Morphodynamics, Obihiro, Japan, p. 525- 534.